

# **Benzene dynamics and biodegradation in alluvial aquifers affected by river fluctuations**

J. Batlle-Aguilar<sup>1,4\*</sup>, B. Morasch<sup>2</sup>, D. Hunkeler<sup>3</sup>, S. Brouyère<sup>1</sup>

<sup>1</sup> Department ArGEnCo, Hydrogeology Unit and Aquapôle, University of Liège, Building 52/3, B-4000 Sart Tilman, Belgium ([Serge.Brouyere@ulg.ac.be](mailto:Serge.Brouyere@ulg.ac.be))

<sup>2</sup> Center for Applied Geoscience (ZAG), University of Tuebingen, Sigwartstr. 16, D-72076 Tuebingen, Germany ([Barbara.Morasch@ifg.uni-tuebingen.de](mailto:Barbara.Morasch@ifg.uni-tuebingen.de))

<sup>3</sup> Centre for Hydrogeology, University of Neuchâtel, Rue Emile-Argand 11, CH-2009 Neuchâtel, Switzerland ([Daniel.Hunkeler@unine.ch](mailto:Daniel.Hunkeler@unine.ch))

<sup>4</sup> currently at National Centre for Groundwater Research and Training (NCGRT), School of the Environment, Flinders University, GPO Box 2100, Adelaide, SA-5001, Australia ([jordi.batlleaguilar@flinders.edu.au](mailto:jordi.batlleaguilar@flinders.edu.au))

Final revised manuscript submitted to Groundwater

19<sup>th</sup> April 2013

1 **Abstract**

2 The spatial distribution and temporal dynamics of a benzene plume in an alluvial aquifer strongly  
3 affected by river fluctuations was studied. Benzene concentrations, aquifer geochemistry  
4 datasets, past river morphology and benzene degradation rates estimated *in situ* using stable  
5 carbon isotope enrichment were analysed in concert with aquifer heterogeneity and river  
6 fluctuations. Geochemistry data demonstrated that benzene biodegradation was on-going under  
7 sulphate reducing conditions. Long-term monitoring of hydraulic heads and characterisation of  
8 the alluvial aquifer formed the basis of a detailed modelled image of aquifer heterogeneity.  
9 Hydraulic conductivity was found to strongly correlate with benzene degradation, indicating that  
10 low hydraulic conductivity areas are capable of sustaining benzene anaerobic biodegradation  
11 provided the electron acceptor ( $\text{SO}_4^{2-}$ ) does not become rate limiting. Modelling results  
12 demonstrated that the groundwater flux direction is reversed on annual basis when the river level  
13 rises up to two meters, thereby forcing the infiltration of oxygenated surface water into the  
14 aquifer. The mobilisation state of metal trace elements such as Zn, Cd and As present in the  
15 aquifer predominantly depended on the strong potential gradient within the plume. However,  
16 infiltration of oxygenated water was found to trigger a change from strongly reducing to oxic  
17 conditions near the river, causing mobilisation of previously immobile metal species and vice  
18 versa. Monitored natural attenuation appears to be an appropriate remediation strategy in this  
19 type of dynamic environment provided that aquifer characterisation and targeted monitoring of  
20 redox conditions is adequate and electron acceptors remain available until concentrations of toxic  
21 compounds reduce to acceptable levels.

22

- 23 *Keywords:* surface water – groundwater interaction; aquifer heterogeneity; hydrogeochemistry;
- 24 organic contaminants; metal trace elements; aquifer remediation.

## 25           **INTRODUCTION**

26   Numerous chemical and metallurgical industries were historically situated close to rivers in order  
27   to facilitate the transport of raw materials and supply process water. Improper disposal of solid  
28   and toxic waste over decades has resulted in numerous heavily polluted brownfields located in  
29   alluvial plains, close to rivers (Schirmer et al. 2006). These sites present major environmental  
30   risks, including groundwater deterioration and contaminant dispersion, particularly through  
31   groundwater discharge into surface water.

32   Benzene is a toxic and carcinogenic monoaromatic hydrocarbon petroleum component, which  
33   combined with its higher solubility in comparison to other hydrocarbons, makes it a serious  
34   threat to environmental health and groundwater quality (Fahy et al. 2006; Rooney-Varga et al.  
35   1999). Although benzene naturally biodegrades under aerobic groundwater conditions (Chiang et  
36   al. 1989; Pruden et al. 2003), aquifers affected by petroleum contaminants are generally  
37   characterised as strongly reducing environments. During the past two decades benzene  
38   biodegradation under anaerobic conditions has been extensively studied, either in laboratory  
39   microcosm batches and column tests (Hunt et al. 1997; Kuhn et al. 1988; Anderson et al. 1998)  
40   or, more recently, in the field using carbon isotope fractionation techniques (Fischer et al. 2007).  
41   Heavy metals are often present in petroleum contaminated aquifers, and have been found to  
42   enhance benzene anaerobic biodegradation due to reduction of metal oxides (Villatoro-Monzón  
43   et al. 2008). Conversely, extreme redox gradients in organic pollutant plumes have the potential  
44   to cause the reverse effect and mobilise previously immobile inorganic species.

45   Either natural or forced infiltration of polluted surface water into aquifers (bank filtration) is  
46   commonly used to adsorb and degrade dissolved contaminants in surface water (Hiscock and  
47   Grischek 2002; Doussan et al. 1998). The opposite process, where clean surface water infiltrates

48 into contaminated aquifers contributing to accelerate or enhancing aquifer contaminant  
49 degradation, has only occasionally been studied (Woessner 2000). Vogel and Grbic-Galic (1986)  
50 provided evidence for enhanced toluene and benzene biodegradation by incorporating  
51 oxygenated water into anaerobic aquifer environments, although their study did not involve any  
52 river influence.

53 Alluvial aquifers are strongly heterogeneous porous media with spatially variable hydraulic  
54 properties that lead to preferential flow and solute transport (Anderson et al. 1999; LaBolle and  
55 Fogg 2001). Aquifer heterogeneity directly affects groundwater dynamics and geochemistry,  
56 patterns of groundwater fluxes, contaminant migration, dispersion and reactivity in the  
57 subsurface (Carleton and Montas 2009; Fritz and Arntzen 2007). Scholl (2000) attributed  
58 discrepancies between observed and modelled BTEX biodegradation rates to variability in  
59 estimates of groundwater flow velocities, with increased discrepancy in areas where  
60 heterogeneity was higher. Heeren et al. (2010) found subsurface physical heterogeneity to be  
61 responsible for preferential flow paths for contaminants but also for causing spatially non-  
62 uniform river – aquifer interaction. Maier et al. (2007) showed the direct influence of aquifer  
63 thickness and aquifer heterogeneity on natural attenuation processes in aquifers. Given that the  
64 thickness of alluvial aquifers can be reasonably determined provided borehole data is available to  
65 the base of the aquifer, aquifer heterogeneity remains the most challenging issue to solve. Such  
66 information is paramount for choosing the most appropriate remediation measure, such as  
67 monitored natural attenuation (Blum et al. 2009), pump and treat systems (Bear and Sun 1998),  
68 or permeable reactive barriers (Hemsi and Shackelford 2006). Aquifer characterisation that  
69 focuses on assessment of the presence and extent of low permeability areas, their contaminant

70 concentration and potential for pollutant degradation is therefore an essential component in the  
71 design of effective remediation strategies.

72 In this paper we analyse the spatial and temporal evolution of a benzene plume and its related  
73 aquifer geochemistry in an alluvial aquifer in concert with fluctuations in the adjacent river level.  
74 We particularly focus on relating the combined effect of aquifer heterogeneity, spatial variability  
75 of hydrogeochemistry, and strong river fluctuations to biodegradation rates quantified in-situ  
76 from carbon stable isotope analysis at multiple piezometers. We explore the co-occurrence effect  
77 of redox conditions caused by benzene biodegradation and the seepage reversal induced by river  
78 fluctuations on the variably mobile and immobile metal trace elements in groundwater. The  
79 ramifications of these processes are illustrated using a contaminated alluvial aquifer where  
80 principal and secondary benzene sources, together with other organic contaminants and metal  
81 trace elements, have mixed over several decades to create a complex contaminated groundwater  
82 environment that is highly responsive to river fluctuations.

### DESCRIPTION OF THE RESEARCH SITE

83  
84 The site is located 15 km upstream the city of Liège (Belgium, EU), an important centre for the  
85 metallurgical industry in Europe during the last century. The brownfield covers an area of  
86 approximately 10 ha, where a coke and gas production factory operated for 62 years from 1922.  
87 In 1984 the factory was abandoned and dismantled. The site is located 25 m from the Meuse  
88 River (Figure 1), which has an average water level at a baseline of 59.4 m a.s.l. (above sea level)  
89 and a water depth of around 8.5 m. Although river level is artificially maintained by a series of  
90 dams, the river level continuously fluctuates with typical daily amplitudes of centimetres and  
91 typical seasonal amplitudes of up to 2 meters during winter and spring.

92 Approximately 4 m of backfill deposits (materials from demolition of buildings, ashes, brick  
93 fragments, and iron pipes) directly overlie 2 m of silt-sand-clay deposits, and 8 m of alluvial  
94 gravels (constituting the alluvial aquifer). The carboniferous shale bedrock at 52 m a.s.l. is  
95 considered to be the impervious lower boundary of the alluvial aquifer. The mean piezometric  
96 water level in the alluvial aquifer is 60 m a.s.l. and the general groundwater flow direction is  
97 towards the Meuse River with a mean hydraulic gradient of 0.3% (Batlle-Aguilar 2008).

98 Soil and groundwater pollution was discovered at the beginning of the 1990's. Soil samples  
99 taken at multiple locations in the brownfield in 1992, 2001 and 2005 identified considerable  
100 contamination of the backfill deposits (0 to 4 m) by mono and polyaromatic hydrocarbons  
101 (BTEX and PAH). At the time when the soil samples were collected, the Belgian soil legislation  
102 defined compound-specific intervention values as a cut-off risk: soils and/or groundwater  
103 concentrations above this value led to mandatory further action, like remediation, engineering  
104 controls and land-use restrictions or monitoring. Most soil samples contained benzene  
105 concentrations that exceeded, by several orders of magnitude, the benzene intervention value in

106 Belgium, fixed at  $0.6 \text{ mg kg}^{-1}$  (SPAQuE 2007). Toluene, ethylbenzene and xylene concentrations  
107 also significantly exceeded their intervention values (fixed at 85, 76 and  $20 \text{ mg kg}^{-1}$ ,  
108 respectively). The results for PAHs were similar, e.g. naphthalene and fluoranthene overshot  
109 their intervention values by several orders of magnitude (fixed at 17 and  $30 \text{ mg kg}^{-1}$ ,  
110 respectively). The heavy metals Zn, Pb, As and Cd, although less abundant than the organic  
111 pollutants, were also found in concentrations close to or slightly above their individual  
112 intervention values.

113 Simultaneously, more than 60 piezometers were sampled across the brownfield, revealing very  
114 high concentrations of benzene (up to  $560,000 \text{ } \mu\text{g L}^{-1}$ ), toluene ( $77,000 \text{ } \mu\text{g L}^{-1}$ ), m-xylene  
115 ( $15,200 \text{ } \mu\text{g L}^{-1}$ ), naphthalene ( $63,000 \text{ } \mu\text{g L}^{-1}$ ) and fluoranthene ( $2,000 \text{ } \mu\text{g L}^{-1}$ ), up to three orders  
116 of magnitude above respective groundwater intervention values. Heavy metals (e.g. As, Cd, Zn,  
117 Pb) were occasionally detected in high concentrations in groundwater samples, although less  
118 frequently than the organic contaminants.



## 119 MATERIALS AND METHODS

### 120 Tracer injection experiments

121 In order to estimate hydrodispersive properties of the alluvial deposits, such as effective porosity  
122 ( $\theta$ ) and longitudinal dispersivity ( $\alpha_L$ ), forced gradient (induced hydraulic) radial-convergent flow  
123 tracer tests were performed, consisting of pumping water from a well while a tracer is added into  
124 adjacent wells. The arrival of the tracer is monitored in the pumping well, obtaining a tracer  
125 breakthrough curve. In a first step (phase I) different salt (nitrate, lithium and iodide) and  
126 fluorescent tracers (naphthionate and uranine) were injected in several piezometers (U5, 7, 6, 1  
127 and 2) located upgradient of the pumped recovery well (P5) (Figure 1). Unexpectedly, none of  
128 the tracers were detected at the pumped recovery well. A second injection of a mix of different  
129 salt (lithium and iodide) and fluorescent (eosin yellowish, naphthionate, sulforhodamine B and  
130 uranine) tracers was performed in an injection piezometer (U15) downgradient from the same  
131 pumped recovery well of injection Phase I (P5). This time, all tracers were recovered (in P5) at  
132 significant rates and generally after short travel times (Figure S1a-b).

### 133 Groundwater flow and solute transport modelling

134 In this study we make use of the calibration results of a numerical groundwater flow and  
135 transport model, developed for the site with MODFLOW-2000 (Harbaugh et al. 2000). The  
136 model was previously presented by Batlle-Aguilar *et al.* (2009), and only a brief summary  
137 covering its main characteristics is presented here. The model extended to a larger part of the  
138 alluvial plain than the contaminated brownfield, in order to avoid influence of self-defined  
139 boundaries in the brownfield site. Upstream and downstream Dirichlet boundary conditions were  
140 set up, while a no flow boundary condition was set up in the limit between the alluvial plain and

141 the shaly up-hill bedrock (Figure 1). A Fourier boundary condition was applied at the limit  
142 between the alluvial plain and the river, so river fluctuations and riverbank effects were  
143 considered. The finite difference model domain had variable grid refinement from  $5\text{ m} \times 5\text{ m}$   
144 inside the brownfield to  $25\text{ m} \times 25\text{ m}$  at the edges of the regional modelled area. More than 3,000  
145 daily groundwater head measurements at 16 monitoring wells located at different distances from  
146 the river and covering the entire site were used during calibration, which was performed using a  
147 combined approach of zonation outside the brownfield and pilot-points (de Marsily et al. 1984)  
148 distributed across the contaminated area. Calibration was accomplished using PEST (Doherty  
149 2008), and modelled groundwater heads showed a correlation coefficient ( $R^2$ ) of 0.967 with  
150 measured ones. Groundwater flow model calibration resulted in a detailed heterogeneous spatial  
151 distribution of the hydraulic conductivity of the alluvial aquifer in the brownfield area (Figure 2).  
152 The hydraulic conductivity values range from  $1 \times 10^{-5}$  ( $\log_{10} -5$ ) to  $5 \times 10^{-3}$  ( $\log_{10} -2.3$ )  $\text{m s}^{-1}$ , with a  
153 distinctive low permeability zone in the eastern part of the brownfield (blue area) near the Meuse  
154 River and several zones of higher hydraulic conductivity (red zones) in the West and North-West  
155 of the brownfield. Modelling results clearly highlight noticeable aquifer heterogeneity in the  
156 brownfield with the potential to influence contaminant transport, dispersion and degradation  
157 rates in the alluvial aquifer.

158 For the purpose of this study a groundwater transport model was built with MT3DMS (Zheng  
159 and Wang 1999) using the previously calibrated groundwater flow model. The transport model  
160 was calibrated by fitting modelled to measured breakthrough curves obtained from field tracer  
161 injections (Figure S1c-d). The dimensions of the groundwater transport model were limited to  
162 the brownfield. At the limit between the alluvial plain and the river Fourier boundary conditions  
163 were applied, while Dirichlet boundary conditions, directly imported from the calibrated

164 groundwater flow model, were considered elsewhere. Variable grid refinement from 0.5 m × 0.5  
165 m in the benzene source to 10 m × 10 m at the limits of the model was applied. Calibration of the  
166 groundwater solute transport model identified the presence of a mobile ( $\theta_m$ ) and an immobile  
167 ( $\theta_{im}$ ) porosity, the later associated with small-scale heterogeneities of the alluvial deposits  
168 attributed to (nearly) immobile water. The groundwater flow and transport model was used to  
169 evaluate the behaviour of the benzene plume from 2005 to 2007, a period for which detailed time  
170 series were available for river and groundwater levels.

### 171 **Riverbanks: past and present morphology**

172 According to historical maps dating from XIX<sup>th</sup> – XX<sup>th</sup> century, the morphology of the Meuse  
173 River has been substantially altered. Historically, a river channel crossed the current brownfield  
174 site. Between 1908 and 1910 the channel was filled up with materials of unknown origin, and  
175 riverbanks were constructed with a conglomerate of concrete and rock to prevent flooding of the  
176 alluvial plain. The position of the former river channel on the brownfield was determined by  
177 overlapping historical and modern maps of the area (Figure 1). The location of the channel  
178 agrees well with the piezometric line contours and the change in the hydraulic gradient at the  
179 former channel location.

180 According to numerical model calibration the hydraulic conductivity of the semipervious  
181 concrete-rock riverbank was  $6.7 \times 10^{-4} \text{ m s}^{-1}$ . This result was in good agreement with the range of  
182 hydraulic conductivities found using STWT1 (Barlow et al. 2000), between  $1.9 \times 10^{-5}$  and  $1.1 \times 10^{-4}$   
183  $\text{m s}^{-1}$ . The STWT1 analytical model calculates the response of an aquifer to a stress created by  
184 river fluctuations using convolution of the river – aquifer system's response.

## Groundwater geochemistry and benzene degradation

The major source area of benzene around piezometer D2bis was located by combining information about the historical locations of industrial waste disposal in the brownfield and the monitored benzene contamination. Secondary sources (with benzene concentrations several orders of magnitude lower) were related to the location of a former benzene recovery (around piezometers U24 and U25), and around piezometer 14, where NAPL (non-aqueous phase liquid) were present. Contaminants trapped locally in the unsaturated zone may leak into the aquifer, especially during rain periods when perched aquifers are formed. However, considering the substantially lower contaminant concentrations in the unsaturated zone in comparison to concentrations in groundwater, this mechanism for contribution to groundwater pollution was considered to be of minor importance.

The source area (nearby piezometer D2bis) is characterised by strongly reducing conditions (Eh - 300 mV), groundwater concentrations of sulphide ( $\text{HS}^-$ ) above  $1 \text{ mg L}^{-1}$  and methane ( $\text{CH}_4$ ) above  $15 \text{ } \mu\text{g L}^{-1}$ . Concentrations of nitrate ( $\text{NO}_3^-$ ) are between 0 and  $3 \text{ mg L}^{-1}$ , clearly below the background concentrations ( $> 15 \text{ mg L}^{-1}$ ) determined upgradient of the contamination area. Closer towards the river, groundwater becomes less reducing to oxic, with positive Eh values (+100 mV) and concentrations of  $\text{NO}_3^-$  close to background values.

Due to its high toxicity and mobility, benzene was considered to be the most problematic contaminant on the site. Benzene biodegradation under strictly reducing conditions and presumably with  $\text{SO}_4^{2-}$  as main electron acceptor was quantified *in situ* using compound-specific carbon isotope analysis (Morasch et al. 2007).  $\delta^{13}\text{C}$  ratios in benzene increased continuously between the source zone (piezometer D2bis) and the piezometers located along the contaminant plume in the strictly reducing part of the aquifer. Based on the  $^{13}\text{C}$  enrichment, 80% of the

208 residual benzene was found to be biodegraded anaerobically with an average half-life of 180  
209 days. The benzene biodegradation rate was quantified to be  $2 \times 10^{-3} \text{ d}^{-1}$  along the preferential  
210 groundwater flow direction towards East/Southeast (Batlle-Aguilar et al. 2009). Towards the  
211 river, where moderately reducing to oxic conditions prevail, no further  $^{13}\text{C}$ -enrichment in the  
212 residual benzene was found. Consequently, the approach could not be used to calculate benzene  
213 degradation under less reducing/oxic conditions in our field site (Morasch et al. 2011).

214           **RESULTS AND DISCUSSION**

215                   **River morphology**

216   The location of the actual in-filled former river channel corresponds to an observable change in  
217   the modelled hydraulic conductivity field of the site (Figure 2). The modelled aquifer  
218   heterogeneity, obtained independently of the historical geomorphological changes of the Meuse  
219   riverbanks, closely reflects these changes and their effect on the aquifer hydraulic conductivity  
220   distribution. Furthermore, it is likely that the spatial distribution of saturated hydraulic  
221   conductivity, and particularly the former river channel, influenced the tracer experiments. The  
222   recovery well P5 and the injection piezometer U15 (phase II) are both located in the relatively  
223   high hydraulic conductivity alluvial deposits of the former river channel, while piezometers 1, 2,  
224   6, 7 and U5 used during injection phase I are located within the low hydraulic conductivity zone  
225   upgradient of the recovery well. It is hypothesised that the individual tracers injected in phase I  
226   remained below their limits of detection in the pumped water in P5 because they travelled slowly  
227   through the low hydraulic conductivity area, and consequently, were strongly dispersed and  
228   diluted before they reached the recovery well. On the contrary, in phase II the migration of the  
229   tracers injected in U15 downgradient of the recovery well was facilitated by the higher hydraulic  
230   conductivities in this area.

231                   **Aquifer geochemistry and benzene biodegradation**

232   Datasets of benzene concentrations and associated parameters including Eh potential,  $\text{SO}_4^{2-}$ , and  
233    $\text{HS}^-$  were examined in concert with the spatial distribution of hydraulic conductivity obtained  
234   from the numerical groundwater flow model calibration, and benzene biodegradation estimated  
235   from stable carbon isotope analysis (Figure 3 and Table S1).

236 As benzene left the major source zone, it was dispersed and preferentially travelled south-  
237 eastwards following the alluvial deposits with higher hydraulic conductivity (Figure 3a). The  
238 biodegradation of benzene and other organic contaminants resulted in strongly reducing  
239 conditions around the main and secondary sources of contamination, particularly close to  
240 piezometer U25 (Figure 3b).  $\text{NO}_3^-$ , the preferred electron acceptor for anaerobic  
241 microorganisms, was depleted around the major benzene source (close to piezometers C3bis and  
242 D2bis) but was present in the vicinity of the river (up to  $7.3 \text{ mg L}^{-1}$  and  $45.5 \text{ mg L}^{-1}$  in  
243 piezometers U10 and U19, respectively).  $\text{SO}_4^{2-}$ , however, appears to be abundant everywhere in  
244 the aquifer indicating that, unlike  $\text{NO}_3^-$ ,  $\text{SO}_4^{2-}$  as electron acceptor is not a limiting factor for  
245 benzene degradation (Figure 3c). The most elevated concentrations of biogenic  $\text{HS}^-$  were  
246 measured in piezometer D2bis, which is located in the major source zone, an area that appears to  
247 be a hotspot for methanogenesis (Figure 3d).

248 In a flow-through system like an aquifer, enrichment in the heavier carbon isotope relative to the  
249 source is indicative of *in situ* biodegradation of the compound not at a single point but between  
250 two points connected in space. Moving away from the source zone, residual benzene ( $\delta^{13}\text{C} = -$   
251  $24.5\%$ ; D2bis) became continuously enriched in the heavier carbon isotope  $^{13}\text{C}$  as  
252 biodegradation occurred during passage through the aquifer. The significant anaerobic  
253 degradation of benzene between the source and the low-permeability zone in the eastern part of  
254 the brownfield towards the Meuse River are evidenced by isotope ratios of  $\delta^{13}\text{C} = -21.5\%$  (e.g.  
255 piezometers 7, 8 and 15, Figure 4a). At first glance there seems to be a clear correlation between  
256 the rate of anaerobic benzene degradation and hydraulic conductivity zones, as illustrated in the  
257 relationship of  $K$  to  $\delta^{13}\text{C}$  (Figure 4a). Since the continuous enrichment of the heavier carbon  
258 isotope integrates benzene degradation between the source and a sampling point downgradient, a

259 general link between the local hydraulic conductivity and microbial activity cannot be drawn that  
260 easily. Nevertheless, the very good observed correlation between K and  $\delta^{13}\text{C}$  suggests that with  
261 the large excess of the electron acceptor  $\text{SO}_4^{2-}$ , microorganisms find favourable conditions for  
262 benzene degradation in the lower hydraulic conductivity areas around piezometers 7, 8, 15 and  
263 U13 (Figure 4a); in other words, low-permeability areas have a significant impact on benzene  
264 remediation. This finding is contrary to the hypothesis presented by Maier et al. (2007), based on  
265 modelling results, that natural attenuation is enhanced in areas where groundwater flow paths  
266 converges, as these zones are characterised by steep gradients that amplify dispersion of mass  
267 fluxes.

268 Unexpectedly, low  $\text{HS}^-$  concentrations in piezometers 7, 8, 15 and U13 appear to contradict the  
269 relationship between local microbial activity and low permeability areas (Figure 4b). However,  
270 less negative Eh potential and lower  $\text{HS}^-$  content around piezometer 7, 8, 15 and U13 may be a  
271 consequence of occasional (but annual) infiltration of oxic surface water into parts of the  
272 brownfield (Figure 4c). As a consequence of this process  $\text{HS}^-$  decreases while Eh increases to  
273 positive values.

274 All the piezometers where  $\delta^{13}\text{C}$  was estimated fall within the 95% confidence interval of a linear  
275 correlation to hydraulic conductivity with a Pearson coefficient as high as 0.832, with the  
276 exception of piezometers P5, C3bis, 11 and 12 (Figure 4a). Piezometer P5 is the only sampling  
277 location at which  $^{13}\text{C}$  enrichment ( $\delta^{13}\text{C} = -23.9\text{‰}$ ) is lower than expected for its hydraulic  
278 conductivity ( $\log_{10} K -4.3 \text{ m s}^{-1}$ ). P5 is located in the area corresponding to the former river  
279 channel of intermediate hydraulic conductivity and geochemically distinct from the highest  
280 hydraulic conductivity area of the aquifer. Conversely, the cluster of piezometers formed by  
281 C3bis, 11 and 12 presents the highest  $^{13}\text{C}$  enrichment in benzene at the site ( $\delta^{13}\text{C} = -20.9\text{‰}$ ;



282 piezometers 11 and 12). These three wells are located in zones of intermediate to high hydraulic  
283 conductivities ( $\log_{10} K \sim -3.5 \text{ m s}^{-1}$ ) and show much higher  $\delta^{13}\text{C}$  ratios than other piezometers  
284 located in zones of similar hydraulic conductivities. Piezometer C3bis is located close to the  
285 major source zone around D2bis and the high  $^{13}\text{C}$  enrichment can be explained by local but very  
286 efficient benzene degradation. Around piezometers 11 and 12 mixing of the main benzene plume  
287 with secondary plumes of substantially different stable isotope composition can explain these  
288 outliers in the hydraulic conductivity - stable isotope correlation. These results emphasize again  
289 that low permeability zones can sustain anaerobic biodegradation of benzene when the electron  
290 acceptor is not rate limiting. Due to the longer residence time of contaminants in comparison to  
291 high hydraulic conductivity areas, niches of efficient anaerobic biodegradation can establish.

292 It is interesting to note that piezometers D3p and D1p, located close to the source area, fall into  
293 the 95% confidence interval between  $\log_{10}K$  and  $\delta^{13}\text{C}$  (Figure 4a), yet groundwater analysed  
294 from these piezometers have low  $\delta^{13}\text{C}$  enrichment and low  $\text{HS}^-$  concentrations (Figure 4b). On  
295 the other hand, D3p has positive Eh values, while negative Eh values were found in D1p (Figure  
296 4c). These apparently contradictory observations may be attributed to the kinetic biodegradation  
297 behaviour of benzene. Nitrate and iron are today nearly depleted across the entire study site,  
298 although nitrate was found at background concentrations of up to  $190 \text{ mg L}^{-1}$  upstream. The site-  
299 specific absence of these compounds implies that benzene biodegradation is occurring today  
300 using  $\text{SO}_4^{2-}$  as electron acceptor, and the  $\text{SO}_4^{2-}$  concentration is far in excess of that required for  
301 this purpose. Historical benzene biodegradation using alternative electron acceptors to  $\text{SO}_4^{2-}$  can  
302 explain the low  $\text{HS}^-$  concentrations together with positive Eh potentials found in some areas,  
303 such as around piezometer D3p.

### **River fluctuations and benzene dynamics**

304  
305 River fluctuations are responsible for the changes in piezometric levels in the alluvial aquifer.  
306 Cross-correlation analyses revealed that rainfall had almost no direct influence on water table  
307 fluctuations on the site (cross correlation coefficient,  $r_k = 0.1$ ), while river fluctuations in the  
308 vicinity of the site were highly correlated to piezometric level fluctuations on the site ( $r_k = 0.9$ ).  
309 Numerical and analytical results indicate that riverbanks of the Meuse River at the study site are  
310 sufficiently permeable to allow strong exchanges between surface water and groundwater.  
311 Exchanges between the aquifer and the river are thus expected to vary over the year according to  
312 river level fluctuations.

313 The benzene dataset available reveals unexpected fluctuations in benzene concentrations by  
314 several orders of magnitude from one sampling period to another, both in piezometers screened  
315 in the upper and deeper part of the gravel aquifer (Figures 5a-b). Most of the piezometers show  
316 high benzene concentrations in 1991, 2001 and 2005, when the sampling was performed during  
317 the summer period (low river levels). In contrast concentrations are generally lower in 1992 and  
318 2006, when sampling took place during the winter period (high river levels). This concept is in  
319 good agreement with findings of Vermeul et al. (2011), who observed that aqueous  
320 concentrations in bores and vertical wellbore flows were significantly impacted by river stage  
321 fluctuations. Similar processes have also been related to groundwater level rises due to rainfall  
322 (Davis et al. 1999).

323 River fluctuations (Figure 6a) during the period 2005-2007 are shown to be responsible for a  
324 highly dynamic river – aquifer system (Figure 6b). During summer and autumn computed Darcy  
325 fluxes are positive, corresponding to groundwater discharge into the river. Over this period of the  
326 year, the river level is relatively constant at its baseline (59.4 m), with river fluctuations in the

327 order of centimetres causing changes in Darcy fluxes of  $\Delta q = 5 \times 10^{-7} \text{ m s}^{-1}$  at the river-aquifer  
328 interface. Despite these changes the water flow direction is constantly from the aquifer to the  
329 river. However, as a direct response to high water levels in the Meuse River during winter and  
330 early spring period, negative Darcy flux values regularly occur, indicating infiltration of river  
331 water into the aquifer. Computed benzene concentrations are presented for control points located  
332 at 25 and 125 m downgradient of the benzene source towards the river (Figure 6c-d). Every  
333 winter-spring the water level of the Meuse River rises by up to 2 metres, which exacerbates the  
334 lateral dispersion of the benzene plume around its source area (Figure 6e). Conversely,  
335 longitudinal dispersion of the benzene plume towards the river is enhanced by low river water  
336 levels, contributing to the formation of a relatively narrow and elongated benzene plume (Figure  
337 6f). Contrasting spatial coverage of the benzene plume at different periods of the year  
338 emphasised the forward and backward movements of the benzene plume as a response to river  
339 fluctuations. This temporal variability of benzene plume dispersion caused by river fluctuations  
340 explains the variation in benzene concentrations from one sampling period to another by several  
341 orders of magnitude. Groundwater sampling over several years is thus likely to produce results  
342 that indicate unexpected shifts in benzene concentrations if the sampling is not performed during  
343 the same season.

#### 344 **Mobilisation of metal trace elements**

345 According to the concept of co-contamination of organic and inorganic compounds,  $\text{HS}^-$  released  
346 by microbial  $\text{SO}_4^{2-}$  reduction reacts with divalent heavy metal ions like Zn and Cd and  
347 immobilises them in the form of metasulphides (Sandrin and Maier 2003), whereas the reduced  
348 form of arsenic As(III) is more mobile, particularly compared to its oxidised As(V) form (Dixit  
349 and Hering 2003). Accordingly, Zn and Cd have been found at low concentrations in the source

350 area and within the plume, where strongly reducing conditions prevail, but they have been found  
351 downgradient of the plume, close to the river. Conversely, As(III) has been observed within the  
352 plume and source area, but never close to the river.

353 Towards the Meuse River, benzene and other mono- and polyaromatic hydrocarbons are barely  
354 observed and the aquifer turns mildly reducing to oxic. It appears that As(III) mobilised close to  
355 the source area and along the plume is partly re-oxidised to a less mobile form (As(V))  
356 downstream of the benzene plume close to the river. On the contrary, immobile reduced Zn and  
357 Cd in the form of precipitated metasulphides are likely to be mobilised if the aquifer  
358 environment changes to mild reducing or oxic. Additionally, Kao and Want (2000) showed that  
359 aerobic fringes, commonly present downgradient of dissolved BTEX groundwater plumes,  
360 contribute to complement benzene degradation. It is hypothesised that benzene degradation in  
361 our site near the river, mainly due to infiltration of oxic surface water, is complemented by these  
362 aerobic fringes. These two processes combined appear to be sufficient to enhance the  
363 immobilisation of As in its oxic form (As(V)) and mobilisation of oxic species of Zn close to the  
364 river. This hypothesis agrees well with available sampling results, showing the presence of Zn  
365 relatively close to the river but not As (Figure S2). Arsenic concentrations are significantly  
366 different nearby the benzene source area and close to the river, where concentrations below the  
367 detection limit were found. Regarding Zn concentrations, the difference between the source area  
368 and close to the river is not that notorious due to an upgradient contamination coming from an  
369 adjacent scrapyard (see piezometer 251 in Figure S2b). Zn concentrations are however high in  
370 piezometers U15, 7 and 8, an area particularly oxic and identified as a preferential infiltration  
371 path for river water following the former river channel.

372

373           **CONCLUSIONS AND REMEDIATION REMARKS**

374   The analysis of benzene concentrations and geochemical datasets in concert with river  
375   fluctuations and benzene biodegradation can be used to obtain a sound understanding of  
376   temporal and spatial benzene plume dynamics. Cost-effective mid- to long-term datasets of  
377   groundwater heads and river water levels form an essential platform for aquifer characterisation  
378   and hence, understanding of solute dynamics. Benzene *in situ* biodegradation (based on stable  
379   carbon isotopes) and independent data (such as past river morphology), supports understanding  
380   of the river-aquifer system and its influence on benzene plume dynamics.

381   Our results emphasize that low permeability zones can sustain benzene anaerobic biodegradation  
382   provided the electron acceptor does not become rate limiting. It is hypothesised that due to  
383   longer residence times in low hydraulic conductivity areas, niches of efficient anaerobic  
384   biodegradation may establish. Furthermore the anaerobic degradation of benzene affects the  
385   mobilisation of some heavy metals but immobilisation of other species, a process that appears to  
386   be reversed by the input of fresh, oxygen-rich, surface water during high river level conditions.

387   Characterisation of contaminated sites is particularly challenging when located close to rivers.  
388   Monitoring networks that do not consider the dynamic nature of both the river and the aquifer are  
389   likely to result in inappropriate or incomplete pictures of the whole river-aquifer system. We  
390   demonstrated that it is essential to perform groundwater sampling when the system is in an  
391   equivalent hydraulic state, e.g. each year in the same season, to avoid unexpected variability in  
392   contaminant concentrations and thereby misleading results. Furthermore, consideration of the  
393   temporal dynamics of such environments and spatial variability of aquifer geochemistry arising  
394   from both aquifer heterogeneity and presence of contaminants are essential to the effective  
395   implementation of remediation measures.

396 Permeable reactive barriers can be used effectively to treat contaminated aquifers (McGovern et  
397 al. 2002), although their performance depends on aquifer heterogeneity and uncertainty in the  
398 reaction mechanism (Eykholt et al. 1999). Effective implementation requires excellent  
399 characterisation of the aquifer, particularly groundwater fluxes. Pump and treat systems have  
400 been effectively used in hydrocarbon contaminated sites (Rabideau and Miller 1994), although  
401 this technique can easily become unaffordable, as large volumes of water are pumped and need  
402 to be treated. Furthermore, efficacy of this technique in contaminant removal has been  
403 recognised to be limited in some particular situations (Voudrias 2001).

404 Monitored natural attenuation (MNA) is an efficient cost-effective remediation technique that is  
405 applied at many contaminated sites where natural conditions meet the essential environmental  
406 requirements for contaminant biodegradation without human intervention (Alvarez and Illman  
407 2006). The technique has low remediation costs, is not intrusive and does not generate large  
408 volumes of contaminated land and water. However longer periods of time are needed to achieve  
409 the desired environmental target and a sound understanding of the plume dynamics, aquifer  
410 geochemistry, heterogeneity and hydrological boundaries of the contaminated site are  
411 imperative. If all the conditions are not properly met and transport of contaminant compounds to  
412 susceptible downgradient receptors is probable, MNA can be bioestimulated (i.e. by adding  
413 electron acceptors) or applied in combination with other techniques (Colombani et al. 2009).  
414 Based on the results obtained and the sound knowledge of river-aquifer dynamics and aquifer  
415 heterogeneity at the study site, MNA appears to be the most suitable measure to apply. The  
416 implementation of this technique would need to be accompanied by a groundwater monitoring  
417 program to ensure  $\text{SO}_4^{2-}$  is not depleted and that redox conditions continue to be favourable for  
418 the enhancement of benzene degradation and immobilisation of heavy metals. This is particularly

419 important at the study site, as the input of fresh and oxidised water, combined with the depletion  
420 of the main electron acceptor of the benzene degradation process, could lead to a serious  
421 environmental issue by mobilizing heavy metals and allowing benzene plume to flow  
422 downgradient into the river.

423 Finally, it is worth noting that information on historical industrial activities at the site and  
424 nearby, as well as morphological changes such as riverbank construction/modification, certainly  
425 helps to explain apparently inconsistent results found during site characterisation and as a  
426 consequence, helps to improve the understanding of the river-aquifer system and associated  
427 contaminant transport.

428 **ACKNOWLEDGEMENTS**

429 This work was supported by the European Union FP6 Integrated Project AquaTerra (project no.  
430 GOCE 505428) under the thematic priority, Sustainable Development, Global Change and  
431 Ecosystems; and by the Belgian Science Policy (BELSPO) through the SSD FRAC-WECO  
432 project no. SD/TE/02A. The work of S. Brouyère was also supported by research grants provided  
433 by the National Funds for Scientific Research of Belgium (FRS-FNRS Project no. 1.5060.12)  
434 and by the University of Liège Research Council. Thanks are due to Chani Welch for editing and  
435 polishing of the English. Johannes Barth and two anonymous reviewers provided useful review  
436 feedback.



437 **REFERENCES**

- 438 Alvarez, P.J.J., and W.A. Illman. 2006. *Bioremediation and natural attenuation: process*  
439 *fundamentals and mathematical models*. John Wiley & Sons. Hoboken, New Jersey,  
440 USA. 609 pp.
- 441 Anderson, M.P., J.S. Aiken, E.K. Webb, and D.M. Mickelson. 1999. Sedimentology and  
442 hydrogeology of two braided stream deposits. *Sedimentary Geology* 129 no. 3-4: 187-  
443 199.
- 444 Anderson, R.T., J.N. Rooney-Varga, C.V. Gaw, and D.R. Lovley. 1998. Anaerobic benzene  
445 oxidation in the Fe(III) reduction zone of petroleum-contaminated aquifers.  
446 *Environmental Science and Technology* 32 no. 9: 1222-1229.
- 447 Barlow, P.M., L.A. DeSimone, and A.F. Moench. 2000. Aquifer response to stream-stage and  
448 recharge variations. II. Convolution method and applications. *Journal of Hydrology* 230  
449 no. 3-4: 211-229.
- 450 Batlle-Aguilar, J. 2008. Groundwater flow and contaminant transport in an alluvial aquifer: in-  
451 situ investigation and modelling of a brownfield with strong groundwater - surface water  
452 interactions, Ph.D thesis. Faculty of Applied Sciences, ArGEnCo department, University  
453 of Liège, Liège (Belgium). 245 pp.
- 454 Batlle-Aguilar, J., S. Brouyère, A. Dassargues, B. Morasch, D. Hunkeler, P. Höhener, L. Diels,  
455 K. Vanbroekhoven, P. Seuntjens, and H. Halen. 2009. Benzene dispersion and natural  
456 attenuation in an alluvial aquifer with strong interactions with surface water. *Journal of*  
457 *Hydrology* 369 no. 3-4: 305-317.

458 Bear, J., and Y. Sun. 1998. Optimization of pump-treat-inject (PTI) design for remediation of a  
459 contaminated aquifer: multi-stage design with chance constraints. *Journal of*  
460 *Contaminant Hydrology* 29 no. 3: 225-244.

461 Blum, P., D. Hunkeler, M. Weede, C. Beyer, P. Grathwohl, and B. Morasch. 2009.  
462 Quantification of biodegradation for o-xylene and naphthalene using first order decay  
463 models, Michaelis-Menten kinetics and stable carbon isotopes. *Journal of Contaminant*  
464 *Hydrology* 105 no. 3-4: 118-130.

465 Carleton, J.N., and H.J. Montas. 2009. Reactive transport in stratified flow fields with idealized  
466 heterogeneity. *Advances in Water Resources* 32 no. 6: 906-915.

467 Chiang, C.Y., J.P. Salanitro, E.Y. Chai, J.D. Colthart, and C.L. Klein. 1989. Aerobic  
468 biodegradation of benzene, toluene, and xylene in sandy aquifer- Data analysis and  
469 computer modeling. *Groundwater* 27 no. 6: 823-834.

470 Colombani, N., M. Mastrocicco, A. Gargini, G.B. Davis, and H. Prommer. 2009. Modelling the  
471 fate of styrene in a mixed petroleum hydrocarbon plume. *Journal of Contaminant*  
472 *Hydrology* 105 no. 1-2: 38-55.

473 Davis, G.B., C. Barber, T.R. Power, J. Thierrin, B.M. Patterson, J.L. Rayner, and Q. Wu. 1999.  
474 The variability and intrinsic remediation of a BTEX plume in anaerobic sulphate-rich  
475 groundwater. *Journal of Contaminant Hydrology* 36 no. 3-4: 265-290.

476 de Marsily, G., G. Lavedan, M. Boucher, and G. Fasanino. 1984. Interpretation of interference  
477 tests in a well field using geostatistical techniques to fit the permeability distribution in a  
478 reservoir model. In *Geostatistics for natural resources characterization*, vol. 2, ed. G.  
479 Verly, M. David, A. G. Journel and A. Marechal, 831-849. D. Reidel Pub. Co.

480 Dixit, S., and J.G. Hering. 2003. Comparison of arsenic(V) and arsenic(III) sorption onto iron  
481 oxide minerals: Implications for arsenic mobility. *Environmental Science & Technology*  
482 37 no. 18: 4182-4189.

483 Doherty, J. 2008. PEST model-independent parameter estimation. User manual and addendum.  
484 Watermark Numerical Computing, 336 pp.

485 Doussan, C., E. Ledoux, and M. Detay. 1998. River-groundwater exchanges, bank filtration, and  
486 groundwater quality: Ammonium behavior. *Journal of Environmental Quality* 27 no. 6:  
487 1418-1427.

488 Eykholt, G.R., C.R. Elder, and C.H. Benson. 1999. Effects of aquifer heterogeneity and reaction  
489 mechanism uncertainty on a reactive barrier. *Journal of Hazardous Materials* 68 no. 1-2:  
490 73-96.

491 Fahy, A., T.J. McGenity, K.N. Timmis, and A.S. Ball. 2006. Heterogeneous aerobic benzene-  
492 degrading communities in oxygen-depleted groundwaters. *FEMS Microbiology Ecology*  
493 58 no. 2: 260-270.

494 Fischer, A., K. Theuerkorn, N. Stelzer, M. Gehre, M. Thullner, and H.H. Richnow. 2007.  
495 Applicability of stable isotope fractionation analysis for the characterization of benzene  
496 biodegradation in a BTEX-contaminated aquifer. *Environmental Science and Technology*  
497 41 no. 10: 3689-3696.

498 Fritz, B.G., and E.V. Arntzen. 2007. Effect of rapidly changing river stage of uranium flux  
499 through the hyporheic zone. *Groundwater* 45 no. 6: 753-760.

500 Harbaugh, A.W., E.R. Banta, M.C. Hill, and M.G. McDonald. 2000. MODFLOW-2000: The  
501 U.S. Geological Survey modular ground-water model. User guide to modularization  
502 concepts and the ground-water flow process. U.S. Geological Survey, 121 pp.

503 Heeren, D.M., R.B. Miller, G.A. Fox, D.E. Storm, T. Halihan, and C.J. Penn. 2010. Preferential  
504 flow effects on subsurface contaminant transport in alluvial floodplains. *Transactions of*  
505 *the ASABE* 53 no. 1: 127-136.

506 Hemsli, P.S., and C.D. Shackelford. 2006. An evaluation of the influence of aquifer heterogeneity  
507 on permeable reactive barrier design. *Water Resources Research* 42 no. 3: W03402.

508 Hiscock, K.M., and T. Grischek. 2002. Attenuation of groundwater pollution by bank infiltration.  
509 *Journal of Hydrology* 266 no. 3-4: 139-144.

510 Hunt, M.J., M.B. Shafer, M.A. Barlaz, and R.C. Borden. 1997. Anaerobic biodegradation of  
511 alkylbenzenes in aquifer material under methanogenic and iron-reducing conditions.  
512 *Bioremediation Journal* 1 no. 1: 53-64.

513 Kao, C.M., and C.C. Wang. 2000. Control of BTEX migration by intrinsic bioremediation at a  
514 gasoline spill site. *Water Research* 34 no. 13: 3413-3423.

515 Kuhn, E.P., J. Zeyer, P. Eicher, and R.P. Schwarzenbach. 1988. Anaerobic degradation of  
516 alkylated benzenes in denitrifying laboratory aquifer columns. *Applied and*  
517 *Environmental Microbiology* 54 no. 2: 490-496.

518 LaBolle, E.M., and G.E. Fogg. 2001. Role of molecular diffusion in contaminant migration and  
519 recovery in an alluvial aquifer system. *Transport in Porous Media* 42 no. 1-2: 155-179.

520 Maier, U., H. Rügner, and P. Grathwohl. 2007. Gradients controlling natural attenuation of  
521 ammonium. *Applied Geochemistry* 22 no. 12: 2606-2617.

522 McGovern, T., T.F. Guerin, S. Horner, and B. Davey. 2002. Design, construction and operation  
523 of a funnel and gate *in-situ* permeable reactive barrier for remediation of petroleum  
524 hydrocarbons in groundwater. *Water, Air, and Soil Pollution* 136 no. 1: 11-31.

525 Morasch, B., P. Höhener, and D. Hunkeler. 2007. Evidence for in situ degradation of mono-and  
526 polyaromatic hydrocarbons in alluvial sediments based on microcosm experiments with  
527 <sup>13</sup>C-labeled contaminants. *Environmental Pollution* 148 no. 3: 739-748.

528 Morasch, B., D. Hunkeler, J. Zopfi, B. Temime, and P. Höhener. 2011. Intrinsic biodegradation  
529 potential of aromatic hydrocarbons in an alluvial aquifer – Potentials and limits of  
530 signature metabolite analysis and two stable isotope-based techniques. *Water Research*  
531 45 no. 15: 4459-4469.

532 Pruden, A., M.A. Sedran, M.T. Suidan, and A.D. Venosa. 2003. Biodegradation of MTBE and  
533 BTEX in an aerobic fluidized bed reactor. *Water Science and Technology* 47 no. 9: 123-  
534 128.

535 Rabideau, A.J., and C.T. Miller. 1994. Two-dimensional modeling of aquifer remediation  
536 influenced by sorption nonequilibrium and hydraulic conductivity heterogeneity. *Water*  
537 *Resources Research* 30 no. 5: 1457-1470.

538 Rooney-Varga, J.N., R.T. Anderson, J.L. Fraga, D. Ringelberg, and D.R. Lovley. 1999.  
539 Microbial communities associated with anaerobic benzene degradation in a petroleum-  
540 contaminated aquifer. *Applied and Environmental Microbiology* 65 no. 7: 3056-3063.

541 Sandrin, T.R., and R.M. Maier. 2003. Impact of metals on the biodegradation of organic  
542 pollutants. *Environmental Health Perspectives* 111 no. 8: 1093-1101.

543 Schirmer, M., A. Dahmke, P. Dietrich, M. Dietze, S. Gödeke, H.H. Richnow, K. Schirmer, H.  
544 Weiß, and G. Teutsch. 2006. Natural attenuation research at the contaminated megasite  
545 Zeitz. *Journal of Hydrology* 328 no. 3–4: 393-407.

546 Scholl, M.A. 2000. Effects of heterogeneity in aquifer permeability and biomass on  
547 biodegradation rate calculations - Results from numerical simulations. *Groundwater* 38  
548 no. 5: 702-712.

549 SPAQuE. 2007. Guide pratique d'utilisation des normes pour le sol et l'eau souterraine (Practical  
550 guide to the use of standards for soil and groundwater). In French. Société Publique  
551 d'Aide à la Qualité de l'Environnement (SPAQuE), 131 pp.

552 Vermeul, V.R., J.P. McKinley, D.R. Newcomer, R.D. Mackley, and J.M. Zachara. 2011. River-  
553 induced flow dynamics in long-screen wells and impact on aqueous samples.  
554 *Groundwater* 49 no. 4: 515-524.

555 Villatoro-Monzón, W., M. Morales-Ibarria, E. Velázquez, H. Ramírez-Saad, and E. Razo-Flores.  
556 2008. Benzene biodegradation under anaerobic conditions coupled with metal oxides  
557 reduction. *Water, Air, and Soil Pollution* 192 no. 1: 165-172.

558 Vogel, T.M., and D. Grbic-Galic. 1986. Incorporation of oxygen from water into toluene and  
559 benzene during anaerobic fermentative transformation. *Applied and Environmental*  
560 *Microbiology* 52 no. 1: 200-202.

561 Voudrias, E.A. 2001. Pump-and-treat remediation of groundwater contaminated by hazardous  
562 waste: can it really be achieved? *Global Nest Journal* 3 no. 1: 1-10.

563 Woessner, W.W. 2000. Stream and fluvial plain ground water interactions: rescaling  
564 hydrogeologic thought. *Groundwater* 38 no. 3: 423-429.

565 Zheng, C., and P.P. Wang. 1999. MT3DMS: a modular three-dimensional multispecies transport  
566 model for simulation of advection, dispersion, and chemical reactions of contaminants in  
567 groundwater systems. Documentation and user's guide. U.S. Army Engineer Research  
568 and Development Center, 202 pp.

569 **FIGURE CAPTIONS**

570 Figure 1. Position of the former river channel associated with the morphology of the Meuse  
571 River before 1908. Piezometric contours correspond to the groundwater survey performed in  
572 April 2006. The arrow indicates groundwater flow direction. Only piezometers and wells  
573 discussed in the paper are labelled.

574 Figure 2. Spatial distribution of the hydraulic conductivity (in  $\log_{10} \text{ m s}^{-1}$ ) resulting from the  
575 transient calibration of the groundwater flow model. The former river channel and the tracer  
576 injection and recovery wells during tracer injection phases I and II are shown, as well as  
577 positions where stable carbon isotope signatures were determined in residual benzene.

578 Figure 3. Measured concentrations of (a) benzene; (b) redox potential; (c) sulphate; and (d)  
579 sulphide, during the sampling period of 2006. Arrow indicates groundwater flow direction. Only  
580 piezometers and wells discussed in the paper are labelled.

581 Figure 4. Correlation of  $\delta^{13}\text{C}$  with (a)  $\log_{10}K$ ; (b)  $\text{HS}^-$ ; and (c) Eh. Dashed lines show the 95%  
582 confidence limit of its correlation. Only piezometers shown as empty circles are considered in  
583 the correlation.

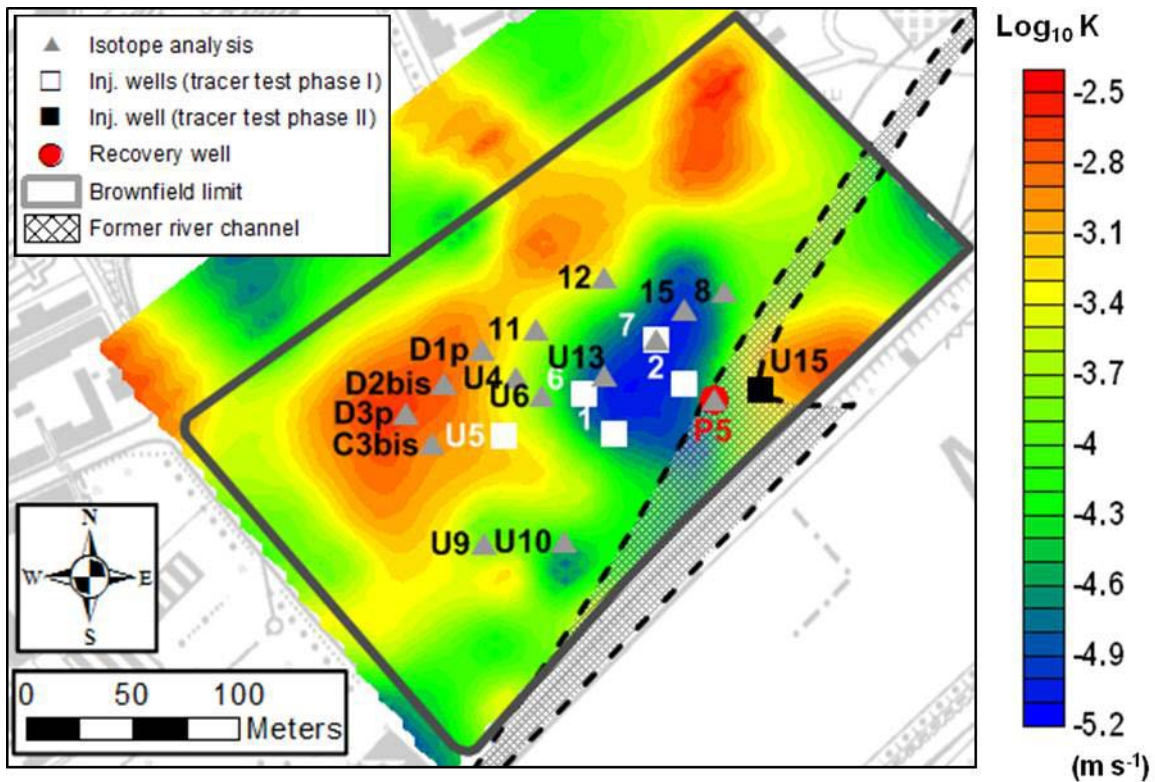
584 Figure 5. Measured concentrations of benzene in groundwater between 1991 and 2006 for all  
585 sampled piezometers screened in the (a) upper; and (b) deeper part of the alluvial aquifer. Red  
586 and blue vertical bars indicate summer-autumn and winter-spring sampling period, respectively.

587 Figure 6. (a) Monitored fluctuations of water levels in the Meuse River; (b) computed Darcy flux  
588 variations at the river-aquifer interface. Modelled benzene concentrations at control points at (c)  
589 25 m; and (d) 125 m downgradient of the benzene source. Computed expansion and narrowing  
590 shape of the benzene plume during (e) high; and (f) low river water level.

591

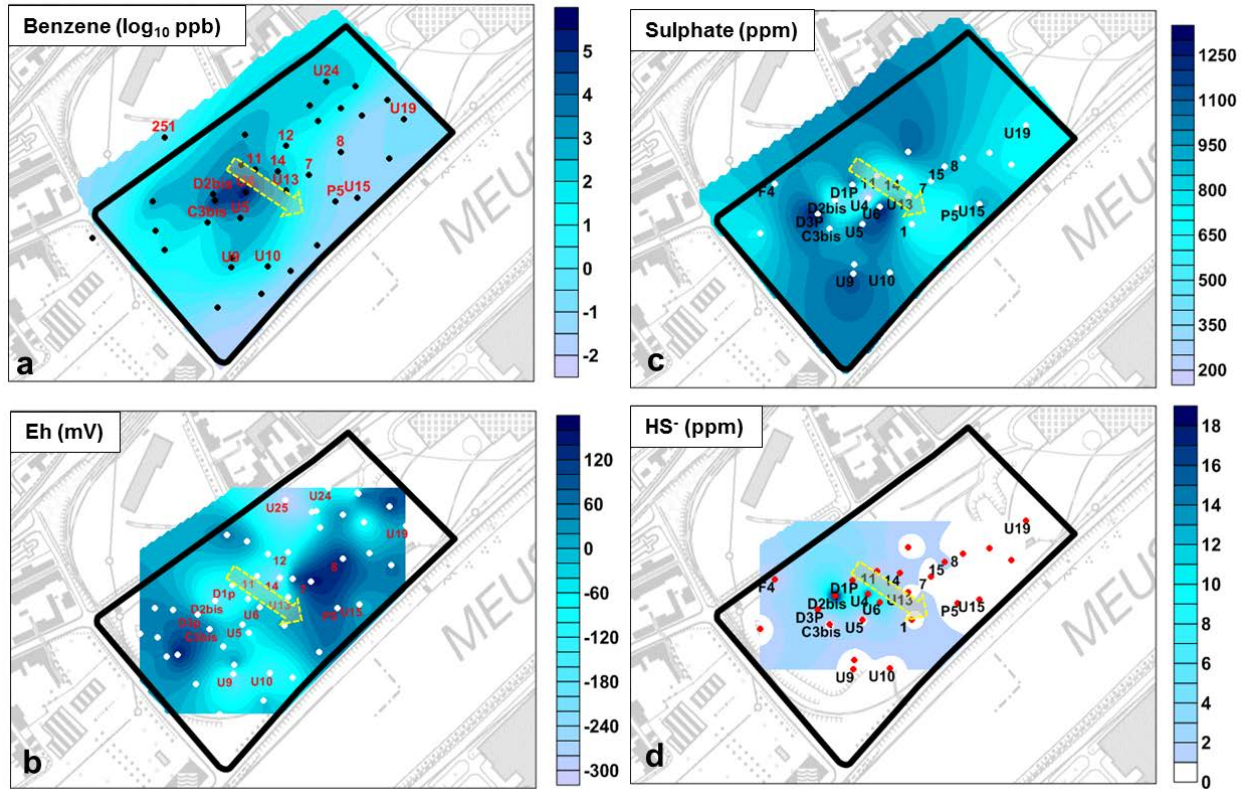






598

599 Figure 2. Spatial distribution of the hydraulic conductivity (in log<sub>10</sub> m s<sup>-1</sup>) resulting from the  
 600 transient calibration of the groundwater flow model. The former river channel and the tracer  
 601 injection and recovery wells during tracer injection phases I and II are shown, as well as  
 602 positions where stable carbon isotope signatures were determined in residual benzene.



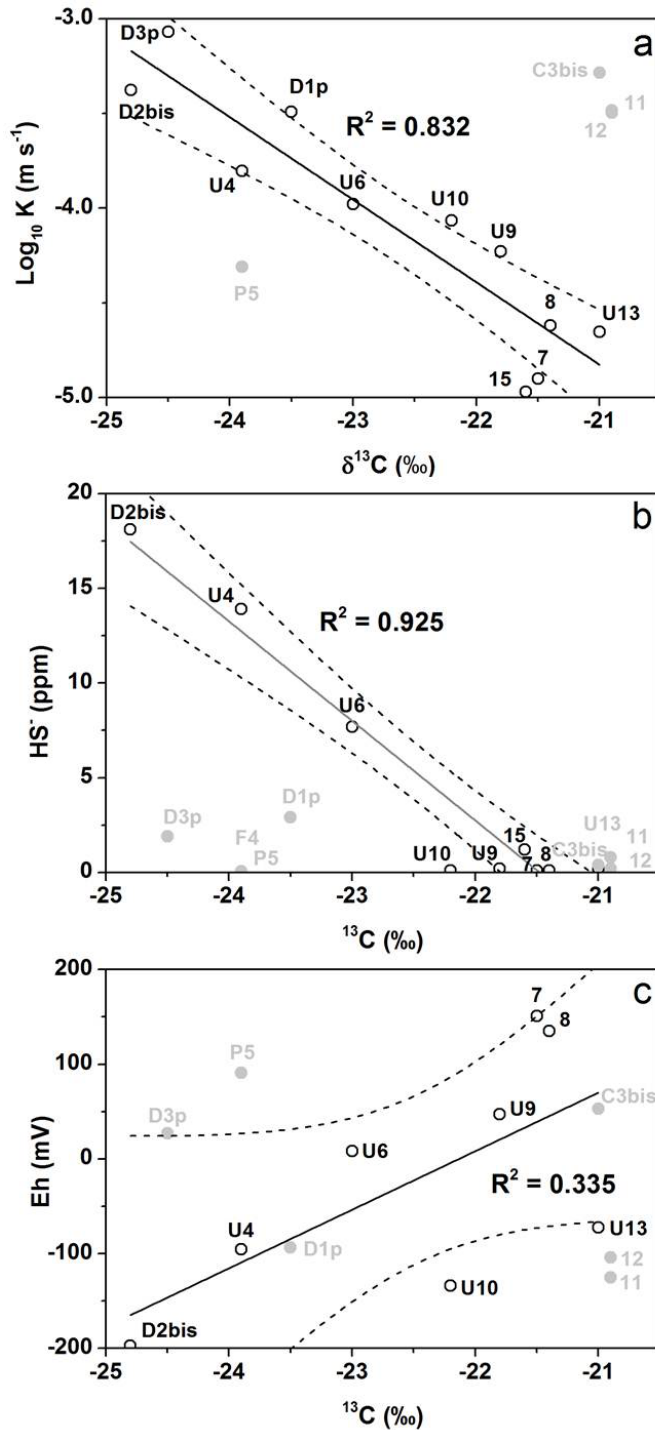
603

604

605 Figure 3. Measured concentrations of (a) benzene; (b) redox potential; (c) sulphate; and (d)

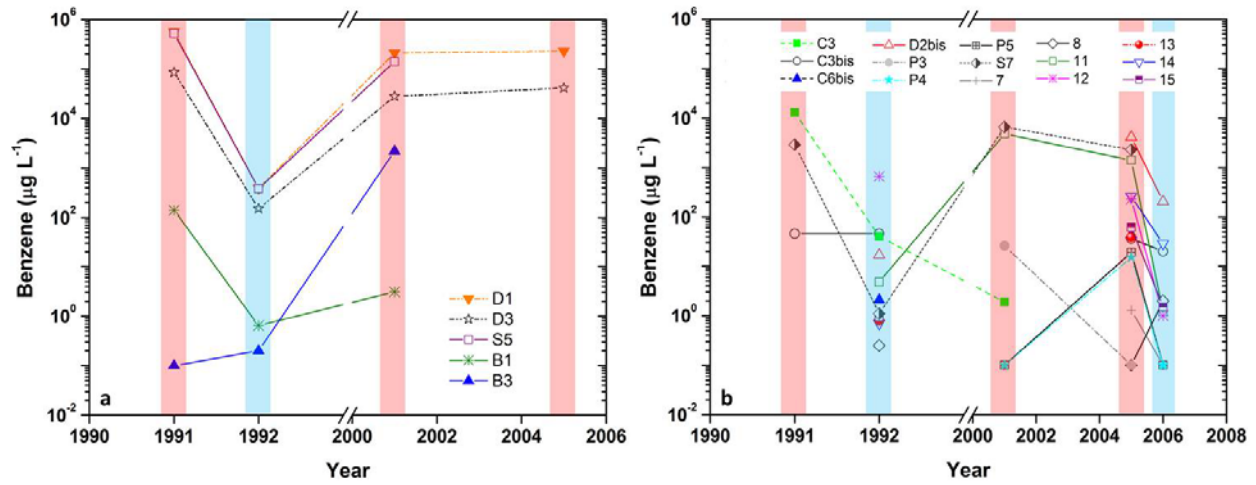
606 sulphide, during the sampling period of 2006. Arrow indicates groundwater flow direction. Only

607 piezometers and wells discussed in the paper are labelled.



608

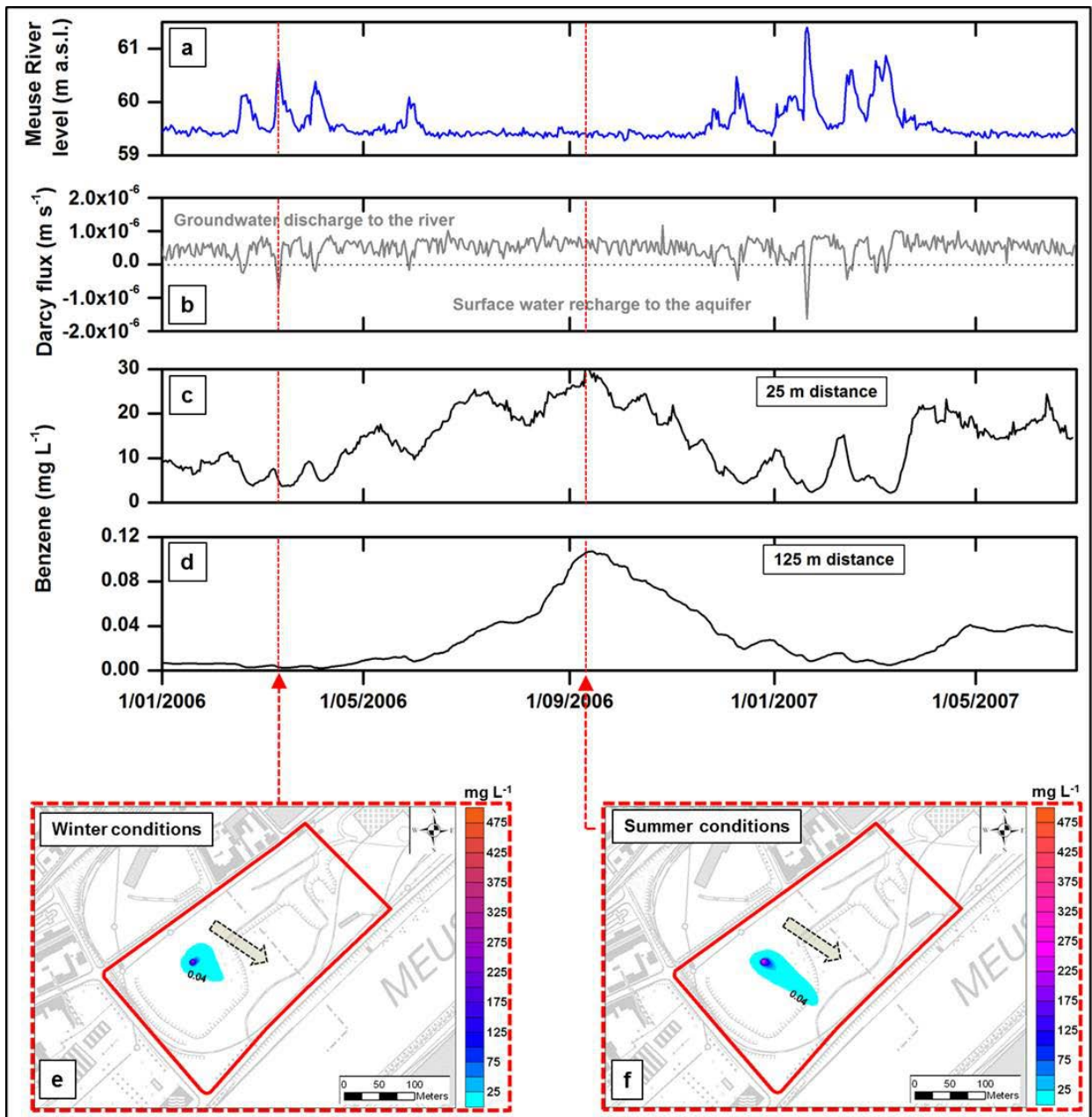
609 Figure 4. Correlation of  $\delta^{13}\text{C}$  with (a)  $\log_{10}K$ ; (b)  $\text{HS}^-$ ; and (c) Eh. Dashed lines show the 95%  
 610 confidence limit of its correlation. Only piezometers shown as empty circles are considered in  
 611 the correlation.



612

613

614 Figure 5. Measured concentrations of benzene in groundwater between 1991 and 2006 for all  
 615 sampled piezometers screened in the (a) upper; and (b) deeper part of the alluvial aquifer. Red  
 616 and blue vertical bars indicate summer-autumn and winter-spring sampling period, respectively.



617

618 Figure 6. (a) Monitored fluctuations of water levels in the Meuse River; (b) computed Darcy flux  
 619 variations at the river-aquifer interface. Modelled benzene concentrations at control points at (c)  
 620 25 m; and (d) 125 m downgradient of the benzene source. Computed expansion and narrowing  
 621 shape of the benzene plume during (e) high; and (f) low river water level.

622